Reduction of Folate by Dihydrofolate Reductase from Thermotoga maritima

Loveridge, E Joel; Hroch, Lukas; Hughes, Robert L; Williams, Thomas; Davies, Rhidian L; Angelastro, Antonio; Luk, Louis Y P; Maglia, Giovanni; Allemann, Rudolf K

Published in:
Biochemistry

DOI:
10.1021/acs.biochem.6b01268

Publication date:
2017

Article

Reduction of Folate by Dihydrofolate Reductase from Thermotoga maritima

E. Joel Loveridge, Lukas Hroch, Robert L. Hughes, Thomas Williams, Rhidian L. Davies, Antonio Angelastro, Louis Y. P. Luk, Giovanni Maglia, and Rudolf K. Allemann

Biochemistry, **Just Accepted Manuscript** • DOI: 10.1021/acs.biochem.6b01268 • Publication Date (Web): 20 Mar 2017

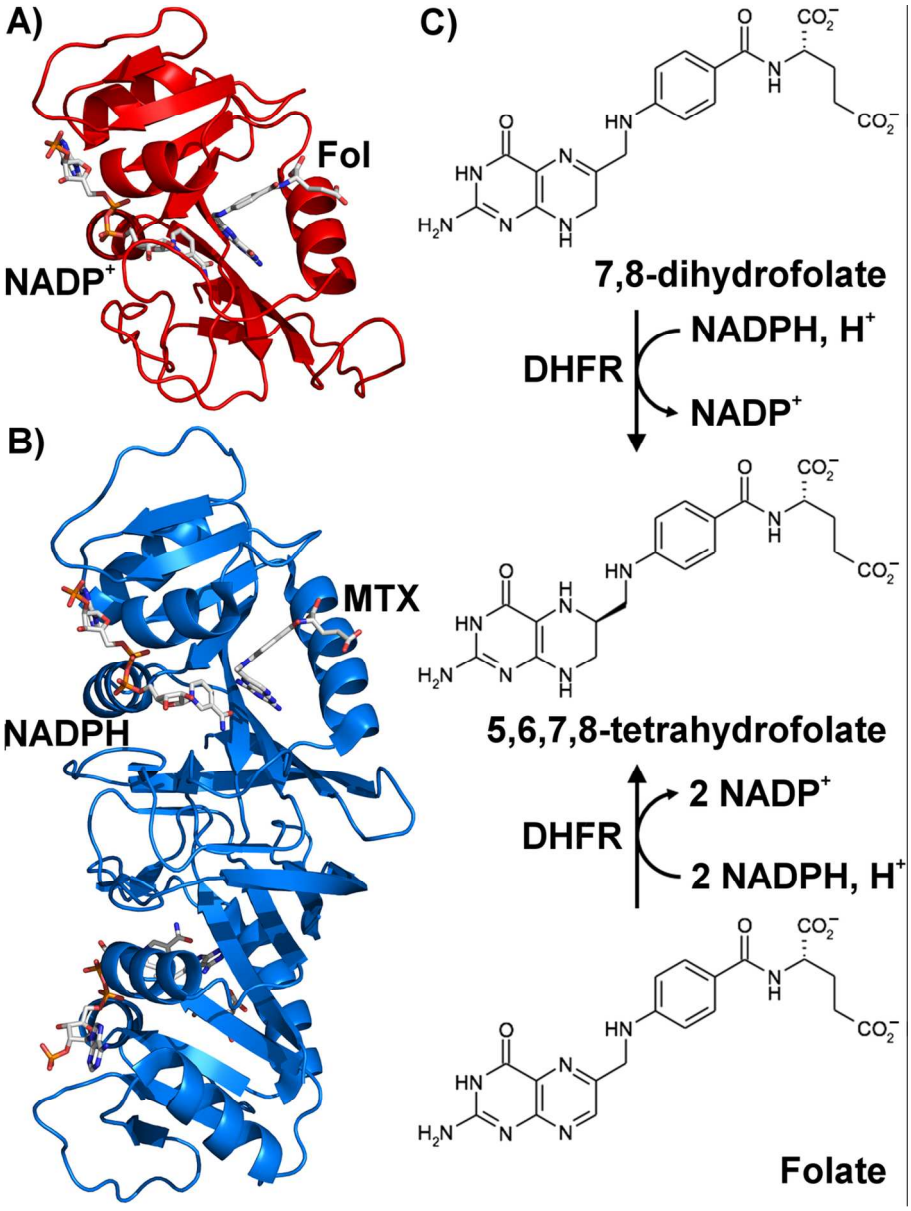

Figure 1. Cartoon representations of the crystal structures of A) EcDHFR (PDB 1RX[24]) and B) TmDHFR (PBD 1D1G[21]), with bound ligands (MTX = methotrexate) shown as sticks, and C) the DHFR-catalysed reduction of dihydrofolate and folate to form tetrahydrofolate.

Figure 1
109x145mm (300 x 300 DPI)

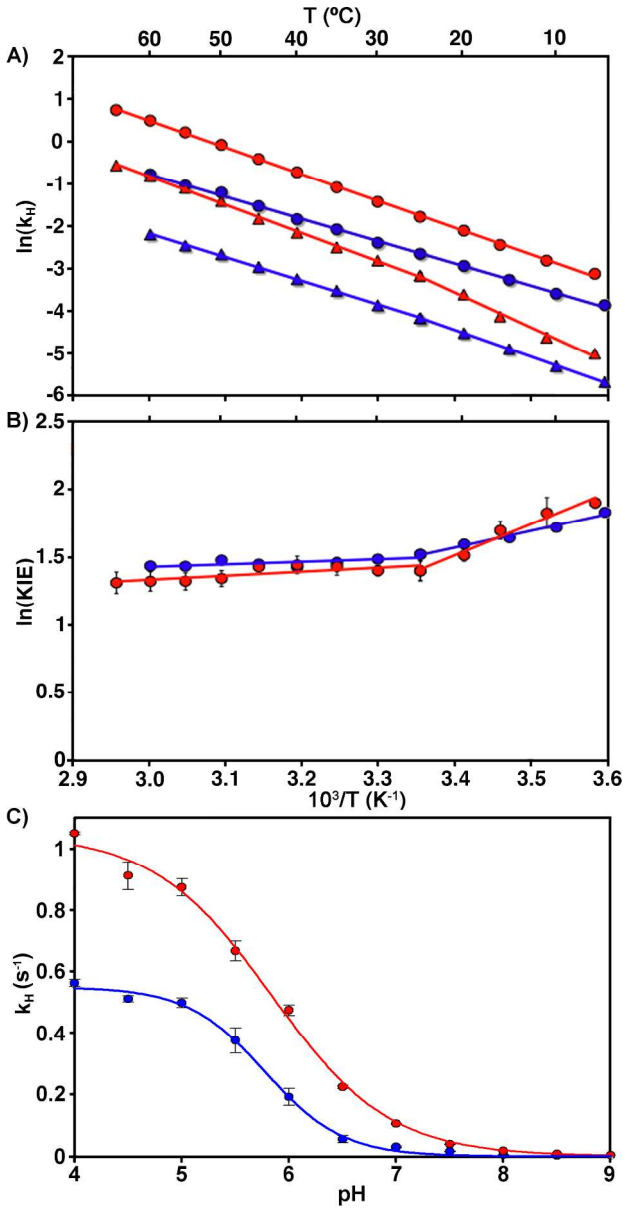

Figure 2. A) Arrhenius plots for hydride (circles) and deuteride (triangles) transfer from NADPH/D to H2F (red)[44] and folate (blue) catalysed by TmDHFR under single-turnover conditions at pH 7, B) plots of the KIE on a logarithmic abscissa against the inverse temperature at pH 7 for H2F (red)[44] and folate (blue), and C) pH dependence of the hydride transfer rate constant at 25 ºC for H2F (red)[55] and folate (blue).
Figure 2
160x314mm (300 x 300 DPI)

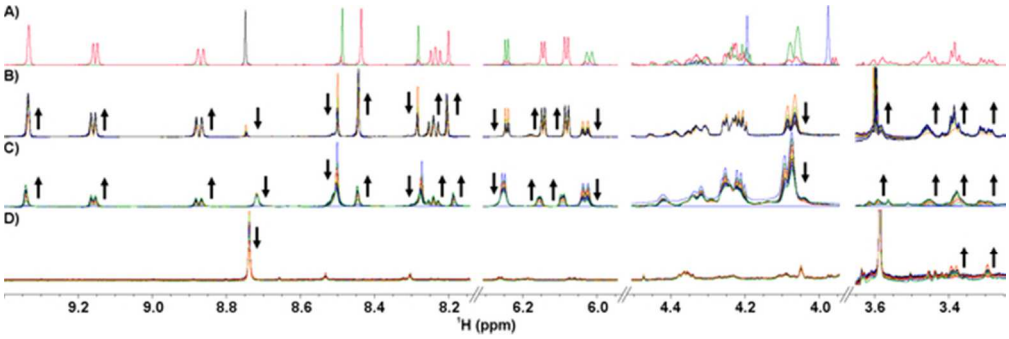

Figure 3. Key regions of the ^{1}H NMR spectra of folate (black), H2F (blue), NADPH (green) and a mixture of NADP+ and H4F (red) (A), and of ^{1}H NMR spectra acquired during reduction of folate using NADPH in the presence of TmDHFR (B) and EcDHFR (C), and using in situ generated NADPD in the presence of TmDHFR (D). In B and D, the sharp singlet at ~3.6 ppm is a ^{13}C satellite from the buffer resonance. The region from 3.25 to 3.65 ppm, which contains the H4F H6, H7 and H9 resonances, is shown at 4x magnification in panels B-D.

Figure 3
55x18mm (300 x 300 DPI)

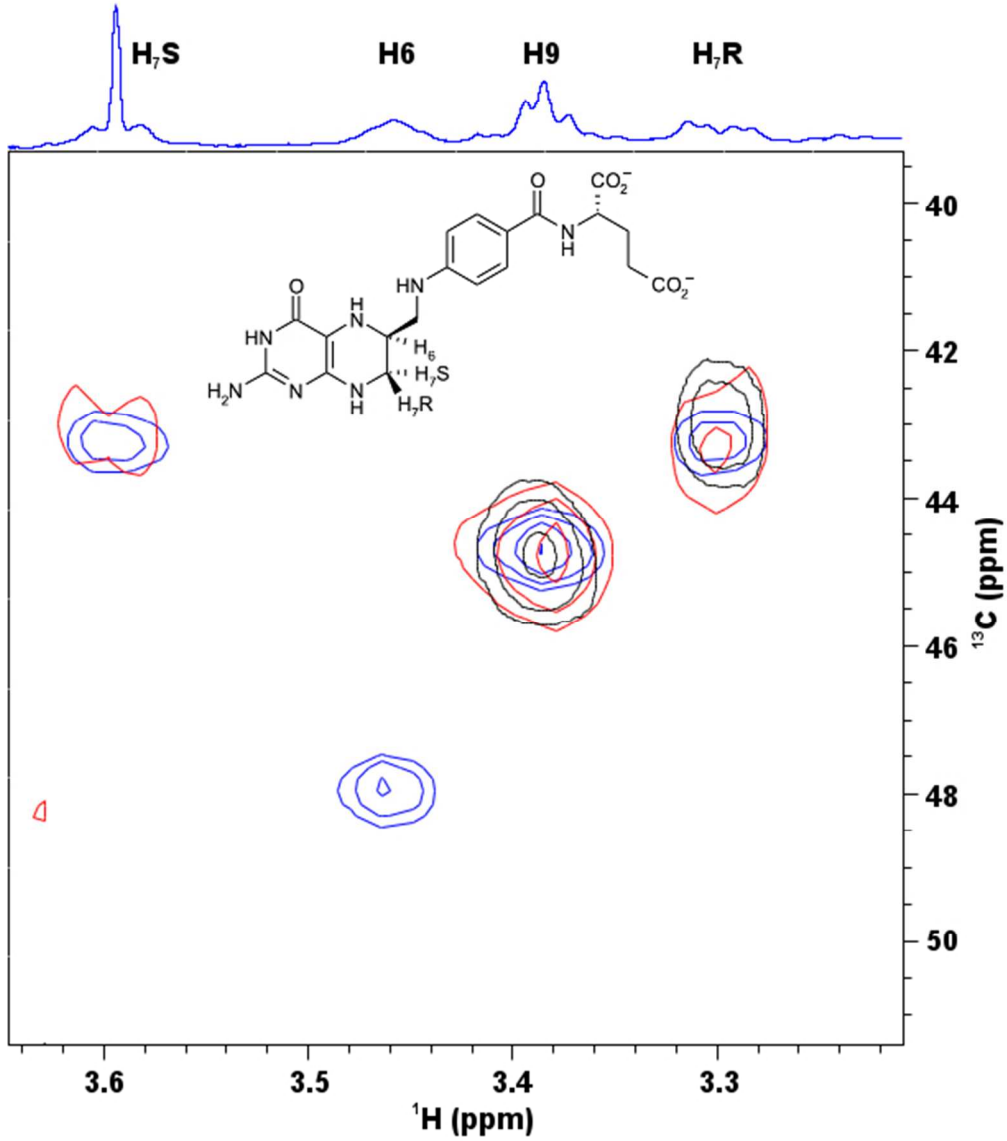

Figure 4. ^{1}H-^{13}C HSQC spectra of the H6/H7/H9 region of tetrahydrofolate produced using TmDHFR with folate and NADPH (blue), EcDHFR with dihydrofolate and NADPD (red), and TmDHFR with folate and NADPD (black). The 1H projection shown is for tetrahydrofolate produced using NADPH, with assignments taken references 32 and 33. The sharp singlet at ~3.6 ppm in the projection is a ^{13}C satellite from the buffer resonance, coincident with the H7S resonance, and is not responsible for the observed cross-peak.

Figure 4

80x91mm (193 x 193 DPI)

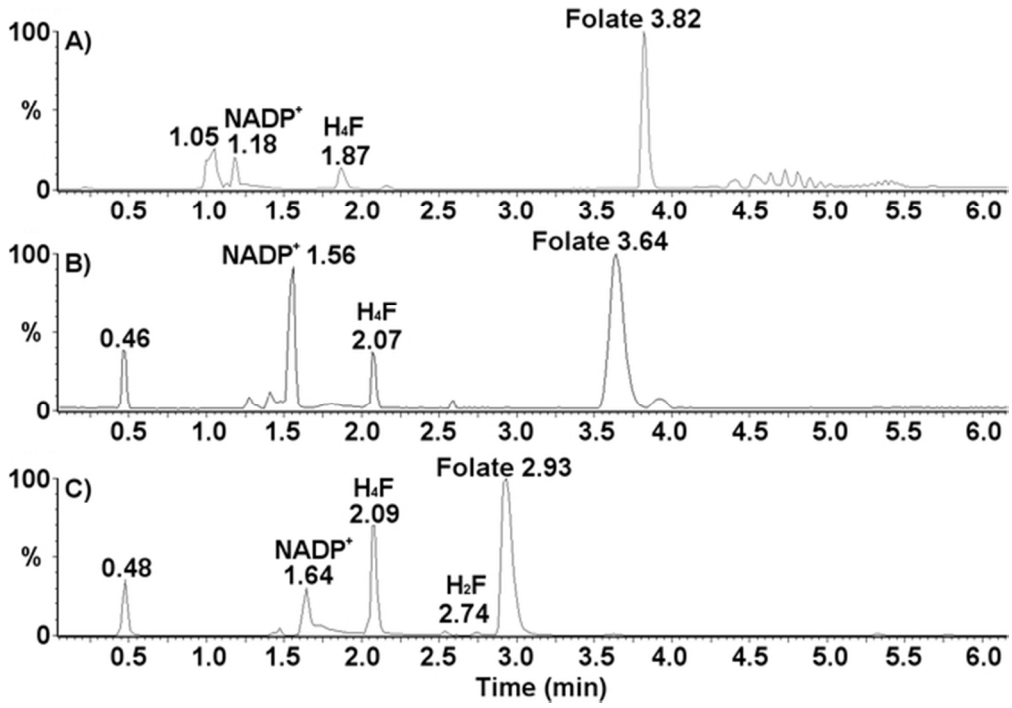

Figure 5. LC-MS analysis of DHFR-catalysed folate reduction. Chromatograms are shown at ~50% completion (by UV) for the reaction catalysed by A) EcDHFR and B) TmDHFR, and C) for reinjection of the TmDHFR post-reaction sample with addition of dihydrofolate. Extracted ion chromatograms and mass spectra are shown in Supplementary Information (Figures S3-S9).

Figure 5
55x38mm (300 x 300 DPI)

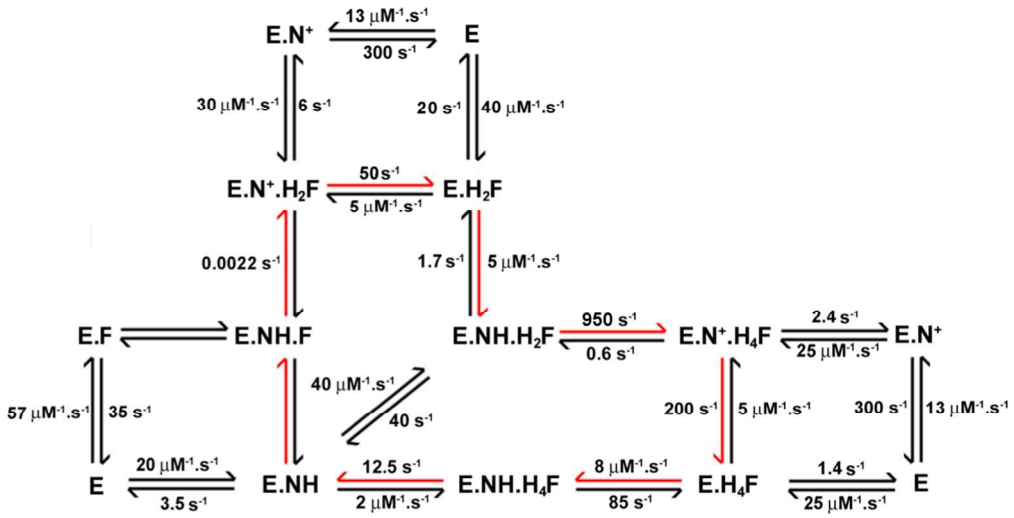

Figure 6. Kinetic scheme for the EcDHFR-catalysed reduction of folate, adapted from references 1 (all values except on/off and hydride transfer rate constants for folate) and 31 (folate on/off rate constants). E represents enzyme (DHFR), NH represents NADPH, N^+ represents $NADP^+$, and F represents folate. The preferred catalytic cycle in the presence of saturating folate and NADPH is highlighted in red.

Figure 6
160x81mm (198 x 198 DPI)

Reduction of Folate by Dihydrofolate Reductase from *Thermotoga maritima*

E. Joel Loveridge,[1,2] Lukas Hroch,[1,3] Robert L. Hughes,[1] Thomas Williams,[1] Rhidian L. Davies,[1,†] Antonio Angelastro,[1] Louis Y.P. Luk,[1] Giovanni Maglia[4,‡] and Rudolf K. Allemann*[1,4]*

1. School of Chemistry, Cardiff University, Main Building, Park Place, Cardiff CF10 3AT, U.K.

2. Department of Chemistry, Swansea University, Singleton Park, Swansea SA2 8PP, U.K.

3. Department of Pharmaceutical Chemistry and Drug Control, Faculty of Pharmacy in Hradec Kralove, Charles University in Prague, Akademika Heyrovskeho 1203, 500 05 Hradec Kralove, Czech Republic

4. School of Chemical Sciences, University of Birmingham, Edgbaston, Birmingham B15 2TT, U.K.

KEYWORDS Dihydrofolate reductase; *Thermotoga maritima*; folate; catalysis.

ABSTRACT. Mammalian dihydrofolate reductases (DHFR) catalyse the reduction of folate more efficiently than the equivalent bacterial enzymes, despite typically having similar efficiencies for the reduction of their natural substrate dihydrofolate. In contrast, we show here that DHFR from the hyperthermophilic bacterium *Thermotoga maritima* is able to catalyse reduction of folate to tetrahydrofolate with a similar efficiency to reduction of dihydrofolate under saturating conditions. NMR and mass spectrometry experiments showed no evidence for production of free dihydrofolate during either the EcDHFR- or TmDHFR-catalysed reductions of folate, suggesting that both enzymes perform the two reduction steps without release of the partially reduced substrate. Our results imply that the reaction proceeds more efficiently in TmDHFR than in EcDHFR because the more open active site of TmDHFR facilitates protonation of folate. Because *T. maritima* lives under extreme conditions where tetrahydrofolate is particularly prone to oxidation, this ability to salvage folate may impart an advantage to the bacterium by minimising wastage of a valuable cofactor.

Dihydrofolate reductase (DHFR) is an essential enzyme in many organisms; it catalyses the NADPH-dependent reduction of 7,8-dihydrofolate (H_2F) to 5,6,7,8-tetrahydrofolate (H_4F). Tetrahydrofolate is required for many one-carbon transfer reactions, most notably in the production of purines, deoxythymidine, glycine, methionine and (in prokaryotes) pantothenic acid. As such DHFR is an important drug target and is a clinical target for antibacterial, antimalarial and anticancer therapies. Almost all known chromosomal DHFRs are monomeric enzymes; the structure, dynamics and kinetics of the prototypic enzyme from *E. coli* (EcDHFR) (Figure 1A) have been extensively studied.[1–20] However, DHFR from the hyperthermophilic bacterium *Thermotoga maritima* (TmDHFR) forms an extremely stable homodimer[21,22] (Figure 1B) with lower catalytic efficiency than monomeric DHFRs.[23,24] Dimerisation is important for the high thermostability of TmDHFR, but in itself dimerisation is not responsible for the lower catalytic activity of TmDHFR compared to monomeric DHFRs.[25–27] Instead, the more open nature of the active site renders the active site less protected from solvent which leads to the reduction in catalytic activity.[21,25–28]

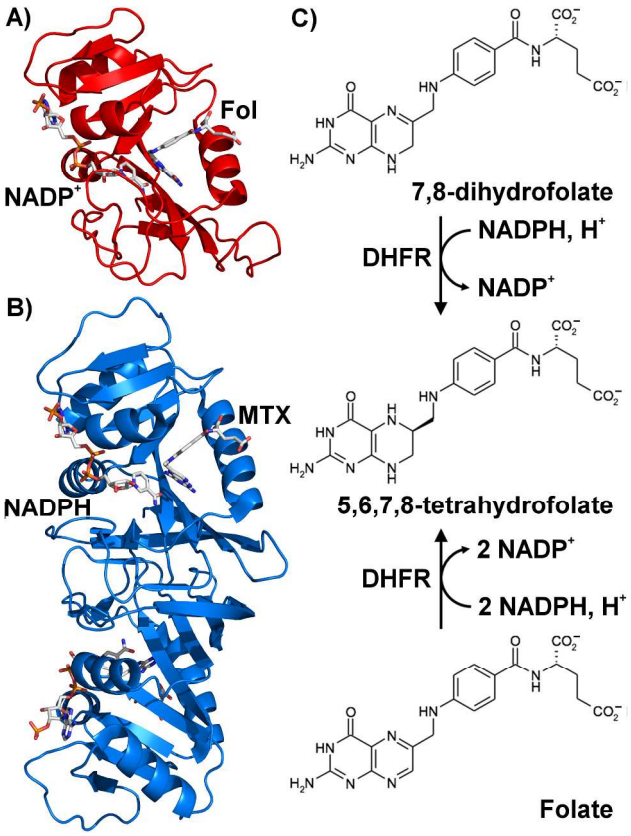

Figure 1. Cartoon representations of the crystal structures of A) EcDHFR (PDB 1RX2[4]) and B) TmDHFR (PBD 1D1G[21]), with bound ligands (MTX = methotrexate) shown as sticks, and C) the DHFR-catalysed reduction of dihydrofolate and folate to form tetrahydrofolate.

Interestingly, vertebrate DHFRs can reduce folate in addition to their natural substrate dihydrofolate.[29] This allows the more stable folate to be used in the supplementation of foods to reduce the incidence of neural tube defects.[30] Bacterial DHFRs, on the other hand, typically do not reduce folate efficiently.[29] The folate specificity of EcDHFR can be increased by introducing loop regions from chicken DHFR.[31]

In X-ray single crystal structures of DHFR, folate and dihydrofolate bind almost identically to the enzyme.[4] Therefore, both molecules present the *Re*-face of the pterin at C6 as the most likely

candidate for attack by the C4 *pro-R* hydride of NADPH (Figure 1B). NMR studies with DHFR from *Lactobacillus casei* (LcDHFR) indeed showed that when folate is fully reduced, both transferred hydrides are present on the same face of the product tetrahydrofolate.[32,33] Because initial reduction at C7 would require both an unfavourable hydride transfer geometry and protonation at the solvent-inaccessible N8, it has been suggested that the initial product of folate reduction is 5,6-dihydrofolate, rather than the natural substrate 7,8-dihydrofolate, and that 5,6-dihydrofolate rearranges to form the more stable 7,8-dihydrofolate, presumably without leaving the active site of the enzyme, prior to the second reduction step.[34–36] This is supported by neutron diffraction studies, which suggest that N5 of folate is protonated in the EcDHFR.$NADP^+$.folate complex.[37] It has been noted, however, that this does not solve the problem of N8 protonation,[34,36] which is still required for the rearrangement of 5,6-dihydrofolate to 7,8-dihydrofolate, and that such apparently unavoidable difficulties in the chemistry are the likely cause of the lower rates of folate reduction compared to dihydrofolate reduction. Here, however, we show that in contrast to other bacterial DHFRs, TmDHFR catalyses reduction of folate with similar efficiency to reduction of dihydrofolate.

MATERIALS AND METHODS

Chemicals. NADPH, $NADP^+$ and isopropyl-β-D-thiogalactopyranoside (IPTG) were purchased from Melford. Folate and $^2H_8$-isopropanol were purchased from Sigma. 7,8-dihydrofolate was prepared by dithionite reduction of folate.[38] EcDHFR,[39,40] TmDHFR,[24,26] NADPD[39] and TbADH[39] were prepared as described previously. Reactant concentrations were determined spectrophotometrically using extinction coefficients of 6,200 cm^{-1} M^{-1} at 339 nm for NADPH and NADPD, and 28,000 cm^{-1} M^{-1} at 282 nm for folate and dihydrofolate.[41]

Steady-state kinetic measurements. Steady state turnover was monitored spectrophotometrically using a JASCO V-660 spectrophotometer by following the decrease in absorbance at 340 nm (ε_{340} (NADPH + substrate) = 11,800 M^{-1} cm^{-1} in both cases)[31,42] in 100 mM potassium phosphate (pH 7.0) containing 100 mM NaCl and 10 mM β-mercaptoethanol. The enzyme (0.05 μM EcDHFR, 0.1-1 μM TmDHFR) was pre-incubated at the desired temperature with NADPH (1-100 μM) for 1 min to avoid hysteresis prior to addition of dihydrofolate or folate (1-100 μM). The change in initial rate with concentration was fit to the Michaelis-Menten equation using SigmaPlot 10. For KIE measurements on k_{cat}, 100 μM each of substrate and cofactor was used. Each data point is the result of three independent measurements.

Pre-steady state kinetic measurements. Single-turnover experiments were performed on an Applied Photophysics stopped-flow spectrophotometer, exciting the sample at 292 nm and observing the loss of fluorescence resonance energy transfer from the enzyme to NADPH during the reaction using a 400 nm cut-off output filter. The enzyme (20 μM final concentration) was pre-incubated with NADPH or NADPD (8 μM final concentration) for at least 5 min in 100 mM potassium phosphate buffer (pH 7.0) containing 100 mM NaCl and 10 mM β-mercaptoethanol. For determining the pH dependence of the single turnover rate constants, MTEN buffer (50 mM morpholinoethanesulfonic acid, 25 mM Tris, 25 mM ethanolamine, 100 mM NaCl and 10 mM β-mercaptoethanol) was used. The reaction was initiated by rapidly mixing in folate (200 μM final concentration) in the same buffer at 20 ºC. Varying the concentrations of the reagents showed that the measured rate constants were limiting values. Each data point is the result of three independent measurements.

NMR experiments. All NMR experiments were performed at 37 ºC on a Bruker AVANCE III 600 MHz (^{1}H) spectrometer with a QCI-P cryoprobe. Spectra were acquired in 100 mM

potassium phosphate buffer (pH 7.0) containing 1 mM NaCl and 10% D_2O, using excitation sculpting for solvent suppression (pulse programme zgesgp). Reference spectra were acquired for NADPH, $NADP^+$, folate and dihydrofolate. A reference spectrum of a mixture of tetrahydrofolate and $NADP^+$ was acquired following incubation of dihydrofolate and NADPH with EcDHFR for five minutes.

The TmDHFR-catalysed reaction was monitored by mixing folate (2.5 mM), NADPH (5 mM, 2 eq.) and TmDHFR (125 μM, 0.05 eq.) in the NMR tube. For the EcDHFR-catalysed reaction 10 mM folate, 20 mM NADPH and 1 mM (0.1 eq.) EcDHFR were used. Solvent-suppressed 1D ^1H spectra (zgesgp) were recorded until no significant change in resonance intensity was observed, and a ^1H-^{13}C HSQC spectrum was then recorded. The reaction catalysed by TmDHFR was performed in 50 mM Tris buffer (pH 7.0) containing 1 mM NaCl and 10% D_2O.

The high salt content of our NADPD led to low-quality NMR spectra. Therefore, to determine the hydride transfer face, a coupled enzyme assay was used to generate NADPD *in situ*. Folate (2.5 mM), TmDHFR (125 μM, 0.05 eq.), TbADH (1 mg of freeze-dried enzyme[39]) and $^2H_8$-isopropanol (25 μL, ~570 μM, 0.23 eq.; also used to provide the lock signal) were mixed in 50 mM Tris buffer (pH 7.0) containing 1 mM NaCl (500 μL final volume). Higher volumes of $^2H_8$-isopropanol caused precipitation over time, which led to poor NMR spectra. The reaction was initiated by addition of $NADP^+$ (250 μM, 0.1 eq.) and solvent-suppressed 1D ^1H spectra (zgesgp) and ^1H-^{13}C HSQC spectra were recorded over 3 hours. Reference ^1H and ^1H-^{13}C HSQC spectra of 6-^2H-tetrahydrofolate were acquired using this coupled assay with dihydrofolate and EcDHFR instead of folate and TmDHFR.

LC-MS analysis. The reaction was also monitored by LC-MS using a Waters Synapt G2-Si time-of-flight mass spectrometer coupled to a Waters Acquity UPLC system with an Acquity

C18 reverse phase column held at 40 ºC throughout the run. Reactions were performed by mixing folate (50 μM), NADPH (100 μM) and TmDHFR (2.5 μM, 0.05 eq.) or EcDHFR (5 μM, 0.1 eq.) in 50 mM Tris buffer, pH 7.0, containing 1 mM NaCl and 10 mM β-mercaptoethanol. Reactions were allowed to proceed to ~50% completion (as determined by UV at 340 nm) before removal of the enzyme using a 12 kDa cut-off filter and injection of 1 μL of the filtrate onto the column. UV spectroscopy showed that folate, dihydrofolate and tetrahydrofolate concentrations were not affected by the filtration step. Compounds were eluted using a gradient of 5-95% aqueous acetonitrile (containing 0.1% formic acid) over 10 minutes, and mass spectra were acquired scanning over m/z 100-1000 in ESP+Ve mode. The reactions and analysis were performed in duplicate. All processing was performed using MassLynx 4.1. Extracted ion chromatograms were taken with m/z 442 and 446 for folate and tetrahydrofolate respectively. For dihydrofolate, ions with m/z 444 and 297 were sought, but not detected, in all chromatograms. To confirm that dihydrofolate was detectable, dihydrofolate (10 μM) was added to a post-LC-MS sample and the analysis repeated.

RESULTS AND DISCUSSION

Steady-state and single-turnover kinetics. Michaelis-Menten kinetics for folate and dihydrofolate were measured with EcDHFR and TmDHFR at 20 °C and pH 7 (Fig. S1). Although, in line with previous observations, EcDHFR gave a k_{cat} with folate ~5000-fold lower than that with dihydrofolate,[31] the k_{cat} for TmDHFR-catalysed folate reduction was only ~3-fold lower than for dihydrofolate (Table 1). The primary kinetic isotope effect (KIE) on TmDHFR-catalysed hydride transfer to folate, obtained by comparing the k_{cat} observed with NADPH with that observed with 4R-(^{2}H)-NADPH (NADPD), was 3.56 ± 0.52. In addition, the single-turnover

rate constant k_H for TmDHFR-catalysed folate reduction, which reports predominantly on the chemical step of the catalytic cycle, was only slightly higher than the steady-state rate constant (Table 1). This demonstrates that the chemical step of the catalytic cycle is predominantly rate limiting, as seen previously for dihydrofolate.[24] Under saturating conditions, TmDHFR is therefore able to reduce folate with a similar efficiency to dihydrofolate. However, as the K_M for folate with TmDHFR is substantially higher than that of dihydrofolate (Table 1), the k_{cat}/K_M for folate is lower than that for dihydrofolate. The reduced affinity for folate relative to that for dihydrofolate seen for TmDHFR is consistent with results obtained with LcDHFR[43] and EcDHFR.[31]

Table 1. Kinetic parameters at 20 ºC for EcDHFR and TmDHFR with H_2F and folate

Enzyme and substrate	K_M / μM	k_{cat} / s^{-1}	k_H / s^{-1}
EcDHFR, H_2F	0.90 ± 0.06	11.1 ± 0.1	159.8 ± 7.9[18]
EcDHFR, folate	8.77 ± 0.70	0.0022 ± 0.0005	ND
TmDHFR, H_2F	< 0.5	0.091 ± 0.02	0.122 ± 0.003[44]
TmDHFR, folate	6.23 ± 0.70	0.0332 ± 0.001	0.053 ± 0.001

The temperature dependence of the primary kinetic isotope effect (KIE) on TmDHFR-catalysed hydride transfer to folate was also determined at pH 7. Single-turnover rate constants

observed with NADPH as cofactor were compared with those observed with NADPD. At all temperatures, the KIE with folate as substrate was not significantly different to that observed previously with dihydrofolate[44] (Figure 2 and Tables S1-S3). Furthermore, the apparent pK_a for the reaction with folate was 5.77 ± 0.03, similar to the value of 5.83 ± 0.06 observed with dihydrofolate[25] (Figure 2 and Table S4). In EcDHFR, the pH dependence of the single-turnover rate constant is determined by the pK_a of protonated dihydrofolate within the active site of the enzyme (6.5), which is elevated substantially from its solution value.[45] Although the pK_a of protonated dihydrofolate within the active site of TmDHFR has not been experimentally verified, the pH dependence of the TmDHFR-catalysed reaction is likely also to be determined by this value. We have previously suggested that the lower apparent pK_a for the TmDHFR-catalysed reaction is due to the more open,[21] and therefore solvent-accessible, active site, which prevents such extensive modulation of the substrate pK_a.[28] As both proposed mechanisms require N8 protonation before the second reduction event, the similar pK_a values for the reactions with folate and dihydrofolate suggest that TmDHFR is able to modulate the pK_a at N8 of folate quite efficiently. It may be that the more solvent-accessible active site in TmDHFR actually facilitates N8 protonation, by providing solvent-mediated routes to protonation and cation stabilisation not available in DHFRs with more tightly closed active sites. A number of crystallographic water molecules are seen in the folate-binding site of TmDHFR in complex with $NADP^+$ and methotrexate (PDB 1D1G), including some buried within the active site pocket.[21] Given the low flexibility and paucity of histidine residues in TmDHFR,[21] a pH dependent conformational change, as seen for apo-EcDHFR,[46] seems less likely.

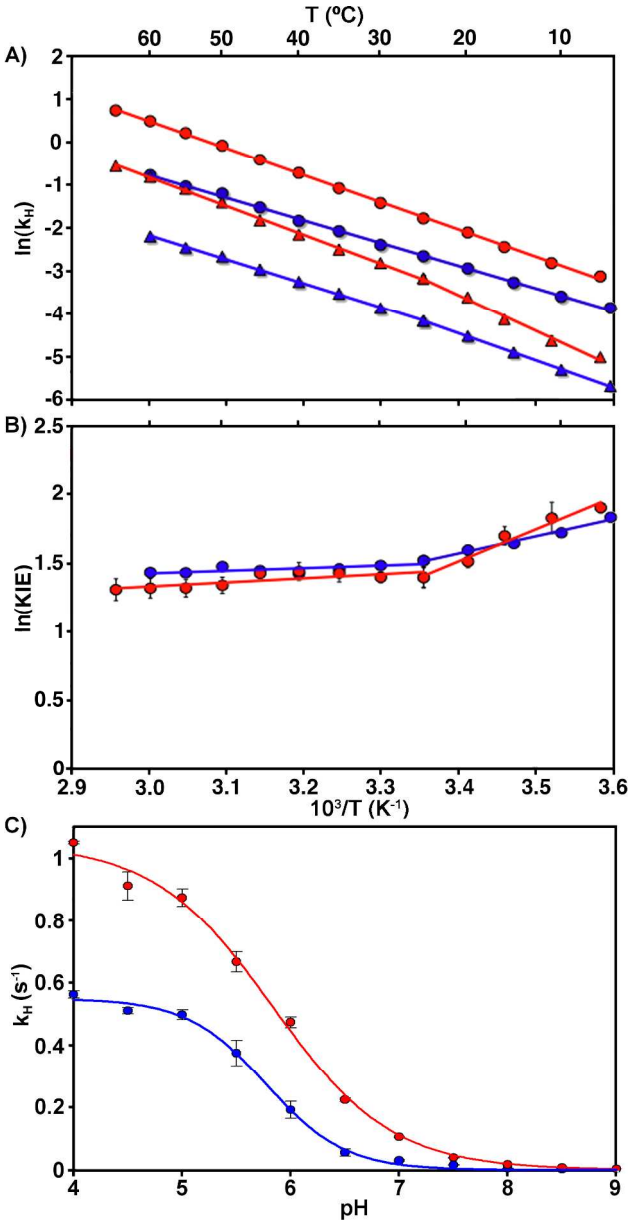

Figure 2. A) Arrhenius plots for hydride (circles) and deuteride (triangles) transfer from NADPH/D to H_2F (red)[44] and folate (blue) catalysed by TmDHFR under single-turnover conditions at pH 7, B) plots of the KIE on a logarithmic abscissa against the inverse temperature at pH 7 for H_2F (red)[44] and folate (blue), and C) pH dependence of the hydride transfer rate constant at 25 ºC for H_2F (red)[55] and folate (blue).

It was not possible to obtain a value for k_H from single-turnover kinetic data with EcDHFR. Although a small loss of fluorescence was observed over short timescales, with rate constant 571.5 ± 43.0 s^{-1} at 20 ºC, a kinetic isotope effect of 1 was observed, demonstrating that the event causing this loss of fluorescence was not the chemical step of the catalytic cycle. A subsequent increase in fluorescence at longer timescales meant that k_H could not be determined.

NMR experiments. NMR experiments were performed to confirm that EcDHFR and TmDHFR convert folate to tetrahydrofolate and to determine whether any free dihydrofolate is produced. EcDHFR-catalysed reduction of dihydrofolate led to loss of the strong singlet resonances for the two H7 and the two H9, and appearance of four new multiplets for H6, $H7_R$, $H7_S$ and the two H9 of tetrahydrofolate as expected[32,33] (Figure 3A).

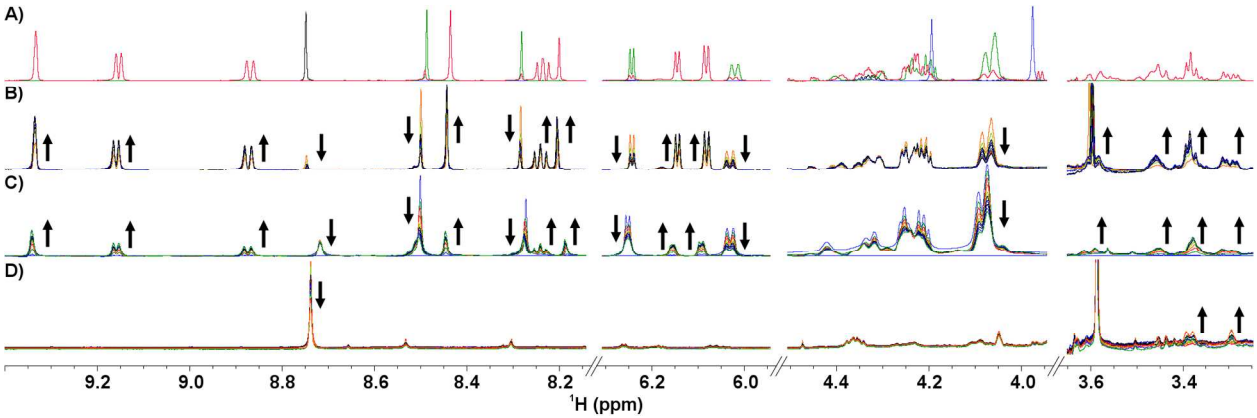

Figure 3. Key regions of the ^{1}H NMR spectra of folate (black), H_2F (blue), NADPH (green) and a mixture of $NADP^+$ and H_4F (red) (A), and of ^{1}H NMR spectra acquired during reduction of folate using NADPH in the presence of TmDHFR (B) and EcDHFR (C), and using *in situ* generated NADPD in the presence of TmDHFR (D). In B and D, the sharp singlet at ~3.6 ppm is a ^{13}C satellite from the buffer resonance. The region from 3.25 to 3.65 ppm, which contains the H_4F H6, H7 and H9 resonances, is shown at 4x magnification in panels B-D.

Incubation of folate and NADPH in the presence of 0.05 equivalents of TmDHFR led to loss of resonances corresponding to these compounds and growth of resonances corresponding to tetrahydrofolate and $NADP^+$ (Figure 3B), confirming that tetrahydrofolate was formed by the TmDHFR-catalysed reduction of folate. For EcDHFR, four-fold higher concentrations of folate and NADPH and 0.1 equivalents of the enzyme were required before useful results could be obtained. Tetrahydrofolate and $NADP^+$ resonances were visible after a few hours, although the folate and NADPH resonances were not greatly diminished (Figure 3C), as expected from the poor efficiency of EcDHFR-catalysed folate reduction. Additional time led to a further decrease in the folate and NADPH resonance intensity and an increase in the $NADP^+$ resonance intensity, although the tetrahydrofolate resonance intensity did not increase further and spectral quality was diminished, presumably due to oxidation of the tetrahydrofolate. For both enzymes, the decrease in integral for NADPH and folate loss, and the increase in integral for $NADP^+$, are proportional to one another (Figures 3B and 3C). As NADPH and folate are present in a 2:1 ratio, this shows that they are depleted in a 2:1 ratio as expected.

No resonances corresponding to dihydrofolate were observed for either enzyme at any time during the experiment (Figure 3). As the reactions were performed with saturating concentrations of NADPH and folate, then if dihydrofolate were released from the enzyme during the catalytic cycle, the high folate concentration would favor folate binding over dihydrofolate re-binding, and consequently more rapid reduction of folate than dihydrofolate. This in turn would lead to a build-up of dihydrofolate. When a 1:1 mixture of folate and dihydrofolate was used, both enzymes preferentially catalysed reduction of dihydrofolate (Figure S2), as expected from our kinetics results. However, the dihydrofolate released from the enzyme is unlikely to successfully

compete with the saturating folate for the active site under the experimental conditions. The NMR experiments therefore strongly suggest that dihydrofolate is not released from the active site of the enzyme.

To determine on which face of folate the two hydride transfers take place, a coupled enzyme assay was used to generate NADPD *in situ*. TmDHFR was incubated with folate in the presence of $NADP^+$, $^2H_8$-isopropanol and alcohol dehydrogenase from *Thermoanaerobacter brockii* (TbADH). Based on our previous work with TmDHFR in organic co-solvents, isopropanol is not expected to have a significant impact on TmDHFR catalysis at the concentrations used,[47] although reaction rates were reduced due to the KIE on the reaction (*vide supra*), leading to poorer tetrahydrofolate signals. As observed previously for LcDHFR,[32,33] signals corresponding to H6 and $H7_S$ were not seen in the ^1H NMR spectrum or the ^1H-^{13}C HSQC of the tetrahydrofolate product (Figure 3D and Figure 4), confirming that hydride transfer to both sites on folate occurred on the same face.

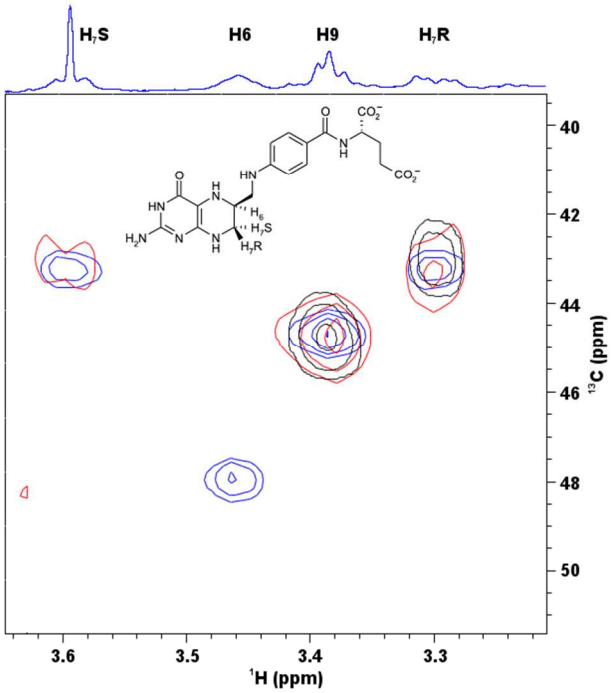

Figure 4. ^{1}H-^{13}C HSQC spectra of the H6/H7/H9 region of tetrahydrofolate produced using TmDHFR with folate and NADPH (blue), EcDHFR with dihydrofolate and NADPD (red), and TmDHFR with folate and NADPD (black). The ^{1}H projection shown is for tetrahydrofolate produced using NADPH, with assignments taken references 32 and 33. The sharp singlet at ~3.6 ppm in the projection is a ^{13}C satellite from the buffer resonance, coincident with the H_7S resonance, and is not responsible for the observed cross-peak.

LC-MS analysis. LC-MS was used to provide further evidence for tetrahydrofolate production without formation of free dihydrofolate. Following incubation of folate and NADPH with TmDHFR and EcDHFR, peaks corresponding to $NADP^+$ and tetrahydrofolate could clearly be observed, although retention times were a little variable between runs (Figure 5, Figures S3-S6). Extracted ion chromatograms revealed no evidence of dihydrofolate (Figures S7-S9). However, repetition of the LC-MS analysis following addition of dihydrofolate showed that this compound could be easily detected by our system (Figure 5C and Figures S7-S9). The sensitivity of LC-MS compared to NMR confirms that no free dihydrofolate is produced during the reduction of folate by either enzyme. As, like the NMR experiments above, these reactions were performed with saturating concentrations of NADPH and folate, this demonstrates that dihydrofolate is not released from the active site of the enzyme.

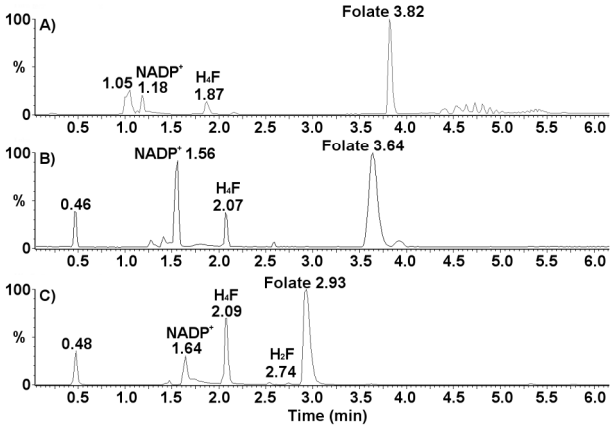

Figure 5. LC-MS analysis of DHFR-catalysed folate reduction. Chromatograms are shown at ~50% completion (by UV) for the reaction catalysed by A) EcDHFR and B) TmDHFR, and C) for reinjection of the TmDHFR post-reaction sample with addition of dihydrofolate. Extracted ion chromatograms and mass spectra are shown in Supplementary Information (Figures S3-S9).

Reduction of folate by EcDHFR and TmDHFR.

For both enzymes, no free dihydrofolate was observed during the reaction. This strongly suggests that dihydrofolate is not released from the active site of either enzyme, but that the catalytic cycle continues *via* release of $NADP^+$ to form the DHFR:H_2F binary complex followed by re-binding of NADPH to form the DHFR:NADPH:H_2F Michaelis complex. This is to be expected for EcDHFR from published kinetic data (Figure 6)[1,31] and from the fact that folate and NADPH were both present in high concentrations in our reactions. In *E. coli*, the concentration of NADPH is 12 μM,[48] higher than the dissociation constant and the Michaelis constant of NADPH,[1,49] and likely still sufficient for NADPH re-binding to be preferred to dihydrofolate loss. Although concentrations of folates[50–52] are likely to be below the Michaelis constant for dihydrofolate,[1,53] this will not affect the preferred catalytic cycle if NADPH concentrations are sufficiently high. Although the intracellular concentrations of NADPH and dihydrofolate in *T.*

maritima are not known, TmDHFR has a higher affinity for the reactants than EcDHFR, making it more likely that the NADPH concentration will be saturating. In addition, the rate constants for binding events in TmDHFR will be even higher than those of release events. The data obtained here also suggest that, as seen for EcDHFR,[1,31] the rate constants for product release from the TmDHFR:$NADP^+$:H_2F and TmDHFR:$NADP^+$:H_4F complexes are substantially smaller than those for $NADP^+$ release.

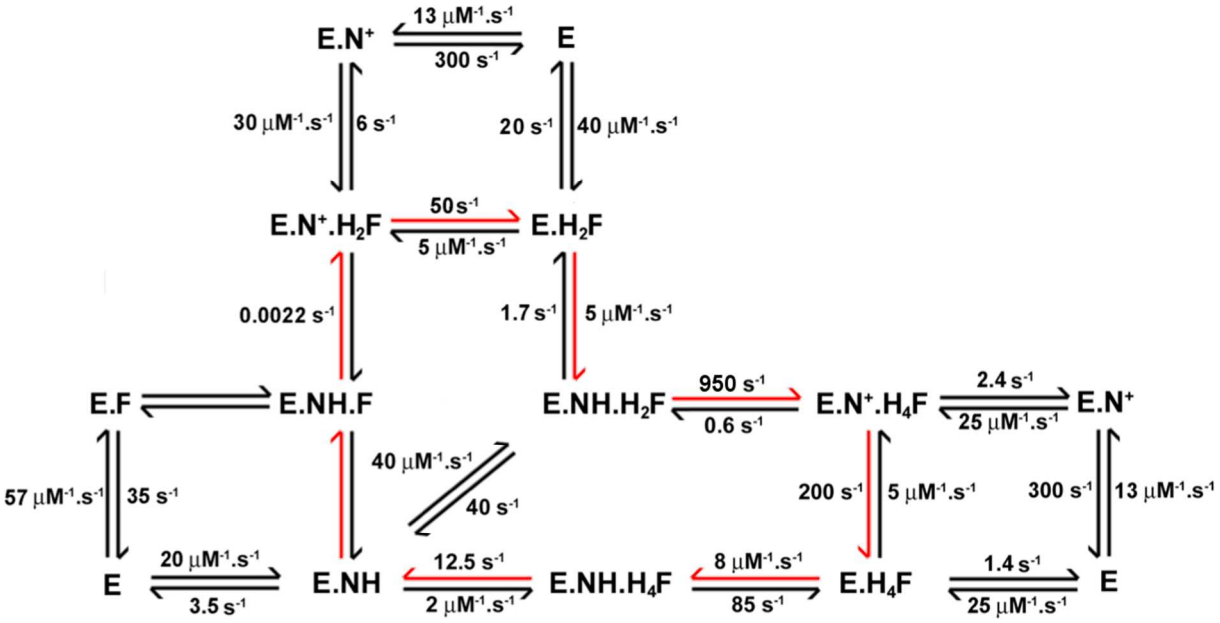

Figure 6. Kinetic scheme for the EcDHFR-catalysed reduction of folate, adapted from references 1 (all values except on/off and hydride transfer rate constants for folate) and 31 (folate on/off rate constants). E represents enzyme (DHFR), NH represents NADPH, N^+ represents $NADP^+$, and F represents folate. The preferred catalytic cycle in the presence of saturating folate and NADPH is highlighted in red.

There are a number of possible explanations for the greater rate of folate reduction by TmDHFR compared to EcDHFR. If the initial reduction occurs at C6, then TmDHFR must be better able to catalyse the rearrangement of 5,6-dihydrofolate to 7,8-dihydrofolate (by N5 deprotonation, 1,2-hydride shift from C6 to C7, and N8 protonation) prior to the second reduction. As both reduction steps show a substantial primary KIE on NADPH oxidation, this rearrangement must be fast compared to the hydride transfer events. Alternatively, if the initial reduction occurs at C7, then TmDHFR must be better able to support the arrangement of reactants required for this, and/or better able to support protonation at N8. The common feature is protonation of N8. As discussed above, the similarity in the apparent pK_a values for the two reduction steps suggests that TmDHFR is able to modulate the pK_a at N8 of folate quite efficiently. It may therefore be that, with its less solvent-accessible active site, EcDHFR fails to modulate the pK_a of folate so efficiently, and rates of folate reduction will be greater at lower pH. Unfortunately, as we were unable to measure a rate constant for EcDHFR-catalysed hydride transfer to folate, we cannot test this.

CONCLUSIONS

TmDHFR catalyses the reduction of folate to tetrahydrofolate with a similar efficiency to the reduction of dihydrofolate under saturating conditions. The similar primary KIE on hydride transfer and its temperature dependence suggest that the nature of the chemical step is similar with the two substrates. Furthermore, no evidence for production of free dihydrofolate was seen for either the EcDHFR- or TmDHFR-catalysed reduction of folate, suggesting that both enzymes perform the two reduction steps without release of partially reduced substrate. It had previously been shown that EcDHFR may be engineered to increase specificity for folate, although this does

not increase the k_{cat},[31] likely because the necessary protonation of folate at N8 is unfavourable within the active site. While our results do not shed light on whether initial reduction of folate occurs at C6 or C7, they suggest that the reaction proceeds more efficiently in TmDHFR than in EcDHFR because the more open active site of TmDHFR facilitates protonation of folate.

The only likely source of folate for *T. maritima* is oxidation of reduced folates. *T. maritima* lives in deep-sea vents and thermal springs, often at temperatures above 90 ºC,[54] and under these conditions the oxidation-prone tetrahydrofolate is particularly vulnerable to degradation. Given that oxidation may also be mediated by species other than O_2, increased efficiency of folate reduction may therefore represent a salvage pathway enabling the bacterium to minimise wastage of this valuable cofactor, thereby gaining an additional competitive advantage under these challenging conditions for life.

ASSOCIATED CONTENT

Supporting Information. Michaelis-Menten curves; additional NMR spectra; mass spectra and extracted ion chromatograms from LC-MS; tabulated data of the temperature dependence of k_H, k_{cat} and the KIE on k_H at pH 7, activation energies and Arrhenius prefactors, and the pH dependence of k_H. This material is available free of charge via the Internet at http://pubs.acs.org.

AUTHOR INFORMATION

Corresponding Author

* To whom correspondence should be addressed. R.K.A.: School of Chemistry, Cardiff University, Main Building, Park Place, Cardiff, CF10 3AT, U.K. Phone: +44 (0)29 2087 9014.

Email: allemannrk@cardiff.ac.uk. E.J.L.: Department of Chemistry, Swansea University, Singleton Park, Swansea SA2 8PP, U.K. E-mail: e.j.loveridge@swansea.ac.uk. Phone: +44 (0)1792 513199.

Present Addresses

† Present address: EQ Ltd Process Consultancy Services, Beechwood House, Christchurch Road, Newport NP19 8AJ, U.K.

‡ Present address: Groningen Biomolecular Sciences and Biotechnology Institute, University of Groningen, Nijenborgh 4, 9747 AG, Groningen, The Netherlands.

Author Contributions

E.J.L., L.H., R.L.H., T.W., R.L.D., A.A., L.Y.P.L. and G.M. all performed experimental work. E.J.L. and R.K.A. wrote the manuscript. All authors have given approval to the final version of the manuscript.

ACKNOWLEDGMENT

This work was supported by the U.K. Biotechnology and Biological Sciences Research Council (BBSRC) through grants BB/E008380/1 and BB/J005266/1 (to R.K.A.), by the U.K. Engineering and Physical Sciences Research Council (EPSRC) through grant EP/L027240/1, by the Life Sciences Research Network Wales (an initiative funded through the Welsh Government's Sêr Cymru programme) (studentship to R.L.H.), by Charles University in Prague (SVV 260 291) and the Erasmus+ programme of the European Union (traineeship and study stay

for L.H.), by the University of Birmingham (studentship to G.M.) and by Cardiff University through a President's Research Scholarship (to A.A.).

ABBREVIATIONS

DHFR, dihydrofolate reductase; EcDHFR, DHFR from *Escherichia coli*; H_2F, 7,8-dihydrofolate; H_4F, 5,6,7,8-tetrahydrofolate; IPTG, isopropyl-β-D-thiogalactopyranoside; LcDHFR, DHFR from *Lactobacillus casei*; $NADP^+$, nicotinamide adenine dinucleotide phosphate; NADPH, nicotinamide adenine dinucleotide phosphate (reduced form); NADPD, 4R-^{2}H-NADPH; TbADH, alcohol dehydrogenase from *Thermoanaerobacter brockii*; TmDHFR, DHFR from *Thermotoga maritima*.

REFERENCES

(1) Fierke, C. A., Johnson, K. A., and Benkovic, S. J. (1987) Construction and Evaluation of the Kinetic Scheme Associated with Dihydrofolate Reductase from Escherichia coli. *Biochemistry 26*, 4085–4092.

(2) Benkovic, S. J., Fierke, C. A., and Naylor, A. M. (1988) Insights into Enzyme Function from Studies on Mutants of Dihydrofolate Reductase. *Science. 239*, 1105–1110.

(3) Gekko, K., Yamagami, K., Kunori, Y., Ichihara, S., Kodama, M., and Iwakura, M. (1993) Effects of point mutation in a flexible loop on the stability and enzymatic function of escherichia coli dihydrofolate reductase. *J. Biochem. 113*, 74–80.

(4) Sawaya, M. R., and Kraut, J. (1997) Loop and subdomain movements in the mechanism of Escherichia coli dihydrofolate reductase: crystallographic evidence. *Biochemistry 36*, 586–603.

(5) Kitahara, R., Sareth, S., Yamada, H., Ohmae, E., Gekko, K., and Akasaka, K. (2000) High pressure NMR reveals active-site hinge motion of folate-bound Escherichia coli dihydrofolate reductase. *Biochemistry 39*, 12789–12795.

(6) Agarwal, P. K., Billeter, S. R., Rajagopalan, P. T. R., Benkovic, S. J., and Hammes-Schiffer, S. (2002) Network of coupled promoting motions in enzyme catalysis. *Proc. Natl. Acad. Sci. U. S. A. 99*, 2794–2799.

(7) Rod, T. H., Radkiewicz, J. L., and Brooks, C. L. (2003) Correlated motion and the effect of distal mutations in dihydrofolate reductase. *Proc. Natl. Acad. Sci. U. S. A. 100*, 6980–6985.

(8) Sikorski, R. S., Wang, L., Markham, K. A., Rajagopalan, P. T. R., Benkovic, S. J., and Kohen, A. (2004) Tunneling and coupled motion in the Escherichia coli dihydrofolate reductase catalysis. *J. Am. Chem. Soc. 126*, 4778–4779.

(9) Boehr, D. D., McElheny, D., Dyson, H. J., and Wright, P. E. (2006) The dynamic energy landscape of dihydrofolate reductase catalysis. *Science (80-.). 313*, 1638–1642.

(10) Wang, L., Goodey, N. M., Benkovic, S. J., and Kohen, A. (2006) The role of enzyme dynamics and tunnelling in catalysing hydride transfer: studies of distal mutants of dihydrofolate reductase. *Philos. Trans. R. Soc. B-Biological Sci. 361*, 1307–1315.

(11) Liu, H. B., and Warshel, A. (2007) The catalytic effect of dihydrofolate reductase and its mutants is determined by reorganization energies. *Biochemistry 46*, 6011–6025.

(12) Thielges, M. C., Case, D. A., and Romesberg, F. E. (2008) Carbon-Deuterium Bonds as Probes of Dihydrofolate Reductase. *J. Am. Chem. Soc. 130*, 6597–6603.

(13) Allemann, R. K., Evans, R. M., and Loveridge, E. J. (2009) Probing coupled motions in

enzymatic hydrogen tunnelling reactions. *Biochem. Soc. Trans. 37*, 349–353.

(14) Loveridge, E. J., Tey, L. H., and Allemann, R. K. (2010) Solvent Effects on Catalysis by Escherichia coli Dihydrofolate Reductase. *J. Am. Chem. Soc. 132*, 1137–1143.

(15) Adamczyk, A. J., Cao, J., Kamerlin, S. C. L., and Warshel, A. (2011) Catalysis by dihydrofolate reductase and other enzymes arises from electrostatic preorganization, not conformational motions. *Proc. Natl. Acad. Sci. 108*, 14115–14120.

(16) Arai, M., Iwakura, M., Matthews, C. R., and Bilsel, O. (2011) Microsecond Subdomain Folding in Dihydrofolate Reductase. *J. Mol. Biol. 410*, 329–342.

(17) Boekelheide, N., Salomon-Ferrer, R., and Miller III, T. F. (2011) Dynamics and dissipation in enzyme catalysis. *Proc. Natl. Acad. Sci. U. S. A. 108*, 16159–16163.

(18) Loveridge, E. J., Behiry, E. M., Guo, J., and Allemann, R. K. (2012) Evidence that a `dynamic knockout' in Escherichia coli dihydrofolate reductase does not affect the chemical step of catalysis. *Nat. Chem. 4*, 292–297.

(19) Weikl, T. R., and Boehr, D. D. (2012) Conformational selection and induced changes along the catalytic cycle of Escherichia coli dihydrofolate reductase. *Proteins Struct. Funct. Bioinforma. 80*, 2369–2383.

(20) Luk, L. Y. P., Ruiz-Pernia, J. J., Dawson, W. M., Roca, M., Loveridge, E. J., Glowacki, D. R., Harvey, J. N., Mulholland, A. J., Tuñón, I., Moliner, V., and Allemann, R. K. (2013) Unraveling the role of protein dynamics in dihydrofolate reductase catalysis. *Proc. Natl. Acad. Sci. U.S.A. 110*, 16344–16349.

(21) Dams, T., Auerbach, G., Bader, G., Jacob, U., Ploom, T., Huber, R., and Jaenicke, R. (2000)

The crystal structure of dihydrofolate reductase from Thermotoga maritima: Molecular features of thermostability. *J. Mol. Biol. 297*, 659–672.

(22) Dams, T., Bohm, G., Auerbach, G., Bader, G., Schurig, H., and Jaenicke, R. (1998) Homo-dimeric recombinant dihydrofolate reductase from Thermotoga maritima shows extreme intrinsic stability. *Biol. Chem. 379*, 367–371.

(23) Wilquet, V., Gaspar, J. A., van de Lande, M., van de Casteele, M., Legrain, C., Meiering, E. M., and Glansdorff, N. (1998) Purification and characterization of recombinant Thermotoga maritima dihydrofolate reductase. *Eur. J. Biochem. 255*, 628–637.

(24) Maglia, G., Javed, M. H., and Allemann, R. K. (2003) Hydride transfer during catalysis by dihydrofolate reductase from Thermotoga maritima. *Biochem. J. 374*, 529–535.

(25) Loveridge, E. J., Rodriguez, R. J., Swanwick, R. S., and Allemann, R. K. (2009) Effect of Dimerisation on the Stability and Catalytic Activity of Dihydrofolate Reductase from the Hyperthermophile Thermotoga maritima. *Biochemistry 48*, 5922–5933.

(26) Loveridge, E. J., and Allemann, R. K. (2010) The Temperature Dependence of the Kinetic Isotope Effects of Dihydrofolate Reductase from Thermotoga maritima Is Influenced by Intersubunit Interactions. *Biochemistry 49*, 5390–5396.

(27) Guo, J., Loveridge, E. J., Luk, L. Y. P., and Allemann, R. K. (2013) Effect of Dimerization on Dihydrofolate Reductase Catalysis. *Biochemistry 52*, 3881–3887.

(28) Loveridge, E. J., Maglia, G., and Allemann, R. K. (2009) The role of arginine 28 in catalysis by dihydrofolate reductase from the hyperthermophile Thermotoga maritima. *ChemBioChem 10*, 2624-2627.

(29) Blakley, R. L. (1969) The Biochemistry of Folic Acid and other Pteridines. Elsevier, New York.

(30) Tamura, T., and Picciano, M. F. (2006) Folate and human reproduction. *Am. J. Clin. Nutr. 83*, 993–1016.

(31) Posner, B. A., Li, L. Y., Bethell, R., Tsuji, T., and Benkovic, S. J. (1996) Engineering specificity for folate into dihydrofolate reductase from Escherichia coli. *Biochemistry 35*, 1653–1663.

(32) Charlton, P. A., Young, D. W., Birdsall, B., Feeney, J., and Roberts, G. C. K. (1979) Stereochemistry of Reduction of Folic Acid Using Dihydrofolate Reductase. *J. Chem. Soc. Commun.* 922–924.

(33) Charlton, P. A., Young, D. W., Birdsall, B., Feeney, J., and Roberts, G. C. K. (1985) Stereochemistry of Reduction of the Vitamin Folic Acid by Dihydrofolate Reductase. *J. Chem. Soc. Trans. 1* 1349–1353.

(34) Gready, J. E. (1980) Dihydrofolate reductase: binding of substrates and inhibitors and catalytic mechanism. *Adv. Pharmacol. Chemother. 17*, 37–102.

(35) Gready, J. E. (1984) Theoretical studies on pteridines. *J. Mol. Struct. THEOCHEM 109*, 231–244.

(36) Gready, J. E. (1985) Theoretical studies on the activation of the pterin cofactor in the catalytic mechanism of dihydrofolate reductase. *Biochemistry 24*, 4761–4766.

(37) Wan, Q., Bennett, B. C., Wilson, M. A., Kovalevsky, A., Langan, P., Howell, E. E., and Dealwis, C. (2014) Toward resolving the catalytic mechanism of dihydrofolate reductase using

neutron and ultrahigh-resolution X-ray crystallography. *Proc. Natl. Acad. Sci. 111*, 18225–18230.

(38) Blakley, R. (1960) Crystalline dihydropteroylglutamic acid. *Nature 188*, 231–232.

(39) Loveridge, E. J., and Allemann, R. K. (2011) Effect of pH on Hydride Transfer by Escherichia coli Dihydrofolate Reductase. *ChemBioChem 12*, 1258–1262.

(40) Hay, S., Evans, R. M., Levy, C., Loveridge, E. J., Wang, X., Leys, D., Allemann, R. K., and Scrutton, N. S. (2009) Are the catalytic properties of enzymes from piezophilic organisms pressure adapted? *ChemBioChem 10*, 2348–53.

(41) Swanwick, R. S., Maglia, G., Tey, L., and Allemann, R. K. (2006) Coupling of protein motions and hydrogen transfer during catalysis by Escherichia coli dihydrofolate reductase. *Biochem. J. 394*, 259–265.

(42) Stone, S. R., and Morrison, J. F. (1982) Kinetic mechanism of the reaction catalyzed by dihydrofolate reductase from Escherichia coli. *Biochemistry 21*, 3757–3765.

(43) Dann, J. G., Ostler, G., Bjur, R. A., King, R. W., Scudder, P., Turner, P. C., Roberts, G. C., and Burgen, A. S. (1976) Large-scale purification and characterization of dihydrofolate reductase from a methotrexate-resistant strain of Lactobacillus casei. *Biochem. J. 157*, 559–571.

(44) Maglia, G., and Allemann, R. K. (2003) Evidence for environmentally coupled hydrogen tunneling during dihydrofolate reductase catalysis. *J. Am. Chem. Soc. 125*, 13372–13373.

(45) Chen, Y. Q., Kraut, J., Blakley, R. L., and Callender, R. (1994) Determination by Raman-Spectroscopy of the Pk(a) of N5 of Dihydrofolate Bound to Dihydrofolate Reductase - Mechanistic Implications. *Biochemistry 33*, 7021–7026.

(46) Chen, Y. Q., Kraut, J., and Callender, R. (1997) pH-dependent conformational changes in Escherichia coli dihydrofolate reductase revealed by Raman difference spectroscopy. *Biophys. J. 72*, 936–941.

(47) Loveridge, E. J., Evans, R. M., and Allemann, R. K. (2008) Solvent Effects on Environmentally Coupled Hydrogen Tunnelling During Catalysis by Dihydrofolate Reductase from Thermotoga maritima. *Chem. - Eur. J. 14*, 10782–10788.

(48) Bennett, B. D., Kimball, E. H., Gao, M., Osterhout, R., Van Dien, S. J., and Rabinowitz, J. D. (2009) Absolute metabolite concentrations and implied enzyme active site occupancy in Escherichia coli. *Nat Chem Biol 5*, 593–599.

(49) Tey, L.-H., Loveridge, E. J., Swanwick, R. S., Flitsch, S. L., and Allemann, R. K. (2010) Highly site-selective stability increases by glycosylation of dihydrofolate reductase. *FEBS J. 277*, 2171–2179.

(50) Bolla, J. R., Su, C.-C., Delmar, J. A., Radhakrishnan, A., Kumar, N., Chou, T.-H., Long, F., Rajashankar, K. R., and Yu, E. W. (2015) Crystal structure of the Alcanivorax borkumensis YdaH transporter reveals an unusual topology. *Nat. Commun. 6*, 6874.

(51) Rohlman, C. E., and Matthews, R. G. (1990) Role of purine biosynthetic intermediates in response to folate stress in Escherichia coli. *J. Bacteriol. 172*, 7200–7210.

(52) Kwon, Y. K., Lu, W., Melamud, E., Khanam, N., Bognar, A., and Rabinowitz, J. D. (2008) A domino effect in antifolate drug action in Escherichia coli. *Nat Chem Biol 4*, 602–608.

(53) Tey, L. H., Loveridge, E. J., Swanwick, R. S., Flitsch, S. L., and Allemann, R. K. (2010) Highly site-selective stability increases by glycosylation of dihydrofolate reductase. *FEBS J.*

277, 2171–2179.

(54) Huber, R., Langworthy, T. A., Konig, H., Thomm, M., Woese, C. R., Sleytr, U. B., and Stetter, K. O. (1986) Thermotoga maritima sp. nov. represents a new genus of unique extremely thermophilic eubacteria growing up to 90 degrees C. *Arch. Microbiol. 144*, 324–333.

(55) Maglia, G., Javed, M. H., and Allemann, R. K. (2003) Hydride transfer during catalysis by dihydrofolate reductase from Thermotoga maritima. *Biochem. J. 374*, 529–535.